Available online at www.sciencedirect.com
SCIENCE DIRECT®
ELSEVIER
Applied Thermal Engineering 24 (2004) 1535–1547
APPLIED THERMAL ENGINEERING
www.elsevier.com/locate/apthermeng

An experimental and numerical study of fluidized bed drying of hazelnuts

Adnan Topuz [a,1], Mesut Gur [b,2], M. Zafer Gul [c,*]

[a] Faculty of Engineering, Department of Mechanical Engineering, University of Zonguldak Karaelmas, 67100 Zonguldak, Turkey
[b] Faculty of Engineering, Department of Mechanical Engineering, University of Sakarya, 54187 Sakarya, Turkey
[c] Faculty of Engineering, Department of Mechanical Engineering, University of Marmara, Goztepe Campus, 81040 Istanbul, Turkey

Received 20 March 2003; accepted 28 November 2003
Available online 17 January 2004

Abstract

The fluidized bed drying of hazelnuts was performed and a laboratory scaled fluidized bed was constructed to obtain experimental data. A mathematical model for the simulation of simultaneous unsteady heat and mass transfer in fluidized bed drying of large particles was performed. Solution of the equation set was carried out by using Crank-Nicholson implicit method within finite volume frame work. A good agreement between the numerical and the experimental results was observed.

Keywords: Fluidized bed; Drying; Hazelnuts; Mathematical model; Validation

1. Introduction

Small particle drying is of importance industrially in the drying of raw materials, intermediates and finished products. Depending on the particle size and nature of feed, the preferred mode of drying is either spray drying, flash drying or fluidized bed drying. While the spray dryers and flash dryers are capable of taking liquid feed, fluidized beds are generally operated with wet solid feed.

* Corresponding author. Tel.: +90-216-348-0292.
E-mail addresses: topuz@karaelmas.edu.tr (A. Topuz), gur@sakarya.edu.tr (M. Gur), gulz1@asme.org, zgul@eng.marmara.edu.tr (M.Z. Gul).
[1] Tel.: +90-372-257-4010; fax: +90-372-257-4023.
[2] Tel.: +90-264-346-0353; fax: +90-264-346-0351.

1359-4311/$ - see front matter
doi:10.1016/j.applthermaleng.2003.11.020

Nomenclature

A	area, m^2
c	specific heat, J/kg °C
D	diffusivity, m^2/s
d	particle diameter, m
E	energy, J
g	gravitational acceleration, m/s^2
H	bed height, m
H_b	heat transfer coefficient of gas and bubble, W/m^3 °C
H_f	bed height after fluidization, m
K_{ib}	mass transfer coefficient of gas and bubble, 1/s
k_p	mass transfer coefficient of particle with gas, m/s
k_t	thermal conductivity, W/m °C
M	moisture content, kg moisture/kg dry solid
Pr	Prandtl number, $Pr = \rho c_p v/k$
r	radial direction, m
Re	Reynolds number, $Re = d_p u \rho_g/\mu_g$
Sc	Schmidt number, $Sc = \mu/\rho D$
T	temperature, °C
u	superficial gas velocity, m/s
V	volume, m^3
x	moisture content, kg moisture/kg dry gas

Greek symbols

α	thermal diffusivity, m/s^2
ε	bed voidage
ρ	density, kg/m^3
v	kinematic viscosity, m^2/s

Subscripts

a	air
b	bubble
i	interstitial gas
g	gas
mf	minimum fluidization
p	particle
ps	particle surface
pw	particle-wall
v	vapor
w	wall
wa	water

Fluidized bed drying among others has the advantage of high intensity of drying and high thermal efficiency with uniform and closely controllable temperature in the bed. It requires less drying time due to high rates of heat and mass transfer and provides for a wide choice in the drying time of the material. The technique offers ease in operation and maintenance of the dryer, adaptability to automation and for combining several processes such as mixing, classification, drying and cooling. The disadvantages, on the other hand, include high pressure drop, attrition of the solids and erosion of the containing surfaces and a possibility of nonuniform moisture content in the product as a result of the distribution of the residence times of individual particles for continuous fluidized bed operations.

Fluidized bed drying of solids can be batchwise or continuous. Batch operation is preferred for small-scale production and for heat sensitive materials. The process conditions are easily selected in batch drying and the product is of uniform quality due to homogeneity of the bed at any instant during its operation. In continuous fluidized drying, product from the dryer under steady-state operation corresponds in its properties to the material within the dryer due to high degree of solids mixing. The residence times of individual particles differ widely within the dryer; hence, the product contains particles dried to different extents. To overcome the drawback, internal baffles are often provided in industrial fluidized dryers of circular cross-section and of rectangular cross-section.

Dimattia et al. [4] performed batch drying of red spring wheat in a fluidized bed. They investigated the effect of bed height, gas velocity, initial moisture content and air temperature on drying rate. Dimattia et al. [5] investigated slugging characteristics of Group D particles (spoutable, large and dense particles, $d_p > 500$ μm) in fluidized beds. Karatas and Battalbey [20] studied on the determination of moisture diffusivity of pistachio nutmeat during drying. Puiggali et al. [11] developed and used an equation to describe the kinetics of air-drying of hazelnuts. They proposed the layer drying equation for drying of hazelnuts. They used it with a fixed deep-bed drier model to obtain a comparison with experimental results. Bhagya and Srinivasan [2] investigated the effect of different methods of drying on the functional properties of enzyme treated groundnut flour. They determined certain functional properties of this flour dried by freeze-drying, spray drying, vacuum shelf drying and drum drying. Liang et al. [9] developed a macadamia nut curing system for improving kernel recovery. Moreira and Arkema [10] developed a moisture desorption model for nonpareil almonds. They determined the drying characteristics of individual almonds and almond parts (hull, shell, nut) at 41.3 and 45.9 °C and 38–8% relative humidity. Erbil [6] studied the prediction of the fountain heights in fine particle spouted bed systems. She proposed a new empirical correlation to predict the fountain heights in spouted bed systems operating with fine particles.

Chandran et al. [3] developed a kinetic model for the drying of solids in fluidized beds, assuming a falling rate period following a constant rate period. They obtained the experimental data using batch and continuous single and spiral fluidized beds. Their results are satisfactorily matched with the assumed drying kinetics and the residence time distribution of solids appropriate for the type of dryer. Abid et al. [1] investigated an experimental and theoretical analysis of the mechanisms of heat and mass transfer during the drying of corn grains in a fluidized bed. Their theoretical analysis of the internal mechanisms of heat and mass transfer has been carried out starting from the model of Luikov, which is based on the irreversible thermodynamics. This model takes into account the transfer of water by diffusion under the influence of a gradient of the concentration in moisture and by thermodiffusion under the influence of a temperature gradient. Thomas and Varma [12] experimentally investigated batch and continuous fluidized bed drying of granular cellular materials at different temperatures and flow rates of the heating medium, particle size and mass of solids.

Ersoy et al. [7] studied solids holdup and made particle velocity measurements in a circulating fluidized bed with secondary air injection. Wang [13] developed a mathematical model for the drying process in a fixed bed dryer. He modeled the drying process in terms of balance equations of masses and energies that result in a hyperbolic system of conservation laws with a source term. He solved this system numerically by an operator splitting technique based on Strang's algorithm. Hajidavalloo and Hamdullahpur [8] proposed a mathematical model of simultaneous heat and mass transfer in fluidized bed drying of large particles. They employed a set of coupled nonlinear partial differential equations to accurately model the process without using adjustable parameters. They used a three-phase model representing a bubble phase, interstitial gas phase and solid phase to describe the thermal and hydrodynamic characteristics of the bed.

Passos and Mujumdar [14] investigated effects of the cohesive force on fluidized and spouted beds of wet particles. Their work aimed to analyze and quantify the differences between the flow behaviors in fluidized and spouted beds of wet and dry particles. Experimentally, they have induced surface stickiness by application of metered amounts of glycerol. In their study, based on pressure drop vs. fluid flow rate curves, solids circulation rates and bed porosity variations, two types of particle–particle interaction forces were identified and their effect on air–solid flow were quantified as a function of glycerol concentration.

Panda et al. [15] have modeled the droplet deposition behavior on a single particle in fluidized bed spray granulation process. Avci et al. [16] investigated the drying process of thin film layers by a theoretical approach. Mhimid et al. [17] have carried out numerical simulation of grain drying in a vertical cylindrical bed with specific boundary conditions; evaporation which occurs with forced air flowing through the bed, has been intensified with a conductive heat flux from the wall. In the experiments, they have heated two side of the fixed bed and considered two mathematical models of heat and mass transfer through granular media: a two-temperature model (No Local Temperature Equilibrium Model: NLTE Model) and a one-temperature model (Local Temperature Equilibrium Model: LTE Model).

In this study, the drying characteristics of the nuts have been investigated in the fluidized bed. The drying process was performed at two different temperatures and velocity of the air in the experiments. A mathematical model for the fluidized bed drying of large particles was employed. Equations were solved by using the Crank-Nicholson implicit numerical method. Numerical results were compared with experimental data.

2. Experimental study

2.1. Physical properties of materials

Hazelnut, which was used in the study as a material to be dried, is approximately spherical in shape. Therefore, hazelnuts were assumed to be spherical with an average diameter of 16 mm. They were separated with two sieves, which have 15 and 17 mm hole diameters. The initial

Table 1
Physical properties of hazelnut [18]

Name	Value	Unit
d_p	16	mm
c_p	1650	J/kg K
ρ_p	795	kg/m^3

moisture contents of hazelnuts are in the range of 7–8 and 21–26% on a dry basis. Other properties of hazelnut can be found in Table 1.

The density of hazelnut was measured and found to be 795 kg/m^3 [19]. The moisture diffusion coefficient of hazelnut is given by Demirtas [21] as follows:

$$D = a\exp(bM_p) \tag{1}$$

where

$$a = 6.0492171 \times 10^{-11}\exp(0.065527T_p) \quad b = 51.218099\exp(-0.016587T_p) \tag{2}$$

In this study, the results of Eq. (1) were employed for new harvested hazelnut. However, this equation is not valid for almost dried grain (moisture content is <8% on a dry basis). In this case, results of this equation were multiplied by 10, to provide a good correlation with the measurement of the diffusion coefficient in the low moisture content range.

2.2. Experimental setup

To investigate the drying characteristics of the hazelnut, a laboratory scale fluidized bed is designed and constructed as shown in Fig. 1. The bed column was made of Plexiglas with 196 mm inner diameter, 1000 mm height and 2 mm wall thickness. A perforated distributor plate with 2 mm thickness and 15 mm holes was used to obtain uniform distribution of the fluidizing air. The air heater consists of four strip electric elements, which has 2000 W total power. The air was provided by a centrifugal blower. The temperature distribution through the bed was measured by a thermometer (Testo 905-T1, Type K thermocouple, 0.1 °C resolution) at different heights above the distributor plate (40, 80, 120 mm above the distributor plate). The pressure difference between the two sides of distributor plate and the distributor plate and fluidized bed height was measured with an electronic pressure cell (Testo 505-P1, 1 mm H_2O resolution). Air velocity was measured and determined with a pitot tube (chromium-plated brass, 350 mm length, 7 mm diameter) and an electronic pressure cell. Inlet and outlet humidity of the air were measured using a humidity measurement stick (Testo 605-H1, 125 mm length, 12 mm diameter, 5–95% RH, 0.1% RH resolution).

The moisture content of the particles was observed by making use of a Sartorius moisture analyzer. Moisture analysis is based on infrared drying. In this process, moisture is removed from the sample by heating. The difference between the initial weight and the final weight yields the moisture content of a sample.

Before each experiment, the unit was run in the absence of particles for about two hours to reach thermal steady state. After the bed reached the required temperature and stabilized, the air

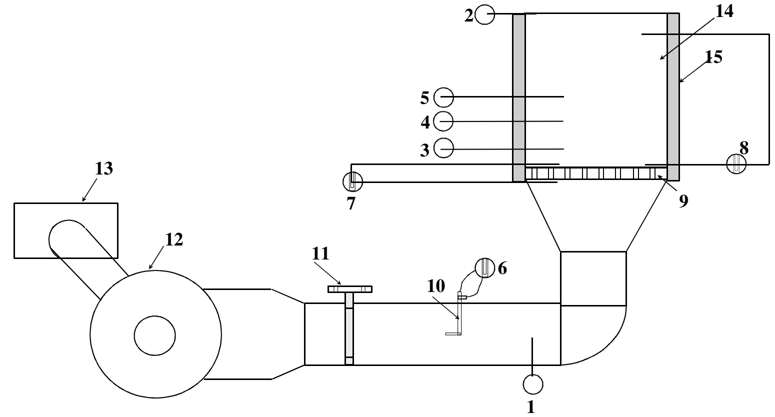

Fig. 1. Schematic diagram of experimental setup (1–2: Humidity stick [for measurement of inlet and outlet air humidity], 3–4–5: thermometers [for measurement of fluidized bed air temperature at 4,8,12 cm of bed, respectively], 6–7–8: pressure cell [for measurement pressure drop. 6: to observe inlet air velocity with pitot tube, 7–8: to measure distributor plate and fluidized bed pressure drop, respectively], 9: perforated plate, 10: pitot tube, 11: valve, 12: fan, 13: climate center, 14: Plexiglas bed column, 15: insulation).

supply and electric heater were turned off and the material was charged into the bed as quickly as possible. The air supply and heater power were then reinstated.

All experiments were conducted under batch fluidization. During the experiments, temperature distribution through the bed and bed pressure drop were measured. As fluidization continued, solid samples were removed from the column at different times and were analyzed for their moisture content.

3. Mathematical model

In this study, a three-phase model proposed by Hajidavalloo and Hamdullahpur [8] representing a bubble phase, gas phase and solid phase was employed to simulate the hydrodynamics of fluidized bed. It can be seen in Fig. 2. They have used this model for fluidized bed drying of corn

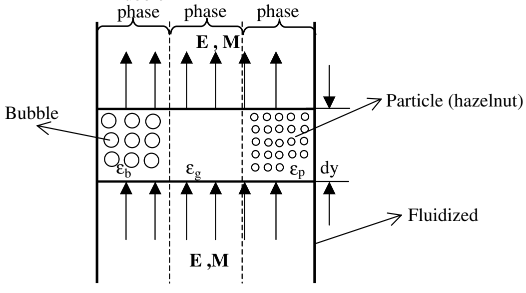

Fig. 2. Sketch of three-phase model.

and wheat particles. The model predictions were satisfactorily verified against a large number of experimental data obtained in their study. This model also predicts the moisture content and temperature distributions within a solid particle without using any adjustable parameters to fit the experimental data. They have observed a good agreement between the numerical and experimental results.

As a preliminary step in modeling, the main features of the bed such as the gas flow rate through the phases, volume fractions and other related parameters must be known. All of these parameters were calculated in a similar manner to the model of Hajidavalloo and Hamdullahpur [8], since hazelnuts, which belong to Group D category, were used as the bed material in this work.

3.1. Bubble phase

The bubble characteristics have an important role in determining the transport phenomena inside the fluidized bed. The size, velocity, moisture content, temperature and interchange coefficient of bubbles depend on its axial position through the bed. The bubbles are considered to be in plug flow with no axial dispersion and contain no particles. Mass balance for the bubble phase can be written as:

$$\frac{\partial}{\partial t}(\rho_a x_b \varepsilon_b) + \frac{\partial}{\partial y}(\rho_a x_b \varepsilon_b u_b) = \rho_a K_{ib}(x_i - x_b) \tag{3}$$

where K_{ib} is the mass transfer coefficient between the bubble phase and the interstitial gas phase:

$$K_{ib} = 4.5\left(\frac{u_{mf}}{d_b}\right) + 5.85\left(\frac{D_v^{1/2} g^{1/4}}{d_b^{5/4}}\right) \tag{4}$$

Energy balance:

$$\frac{\partial}{\partial t}(\rho_a c_b \varepsilon_b T_b) + \frac{\partial}{\partial y}(\rho_a c_b \varepsilon_b u_b T_b) = H_{ib}\varepsilon_b(T_i - T_b) + \rho_a K_{ib}\varepsilon_b(x_i - x_b)c_v(T_i - T_b) \tag{5}$$

and energy transfer coefficient between the bubble phase and the interstitial gas phase H_{ib};

$$H_{ib} = 4.5\left(\frac{u_{mf}\rho_a c}{d_b}\right) + 5.85\frac{(k_{ta}\rho_a c)^{1/2} g^{1/4}}{d_b^{5/4}} \tag{6}$$

3.2. Interstitial gas phase

The interstitial gas phase has interactions with the solid phase, bubble phase and the surface of bed column. A plug flow model can be considered for the interstitial gas phase. Mass balance for this phase:

$$\frac{\partial}{\partial t}(\rho_a x_i \varepsilon_i) + \frac{\partial}{\partial y}(\rho_a x_i \varepsilon_i u_i) = \rho_a k_p(x_p - x_i)6\frac{\varepsilon_p}{d_p} + \rho_a K_{ib}\varepsilon_b(x_b - x_i) \tag{7}$$

Interchange coefficient between solid phase and interstitial gas phase can be written as:

$$k_p = \frac{D_v}{d_p}(2 + 1.8Re^{1/2}Sc^{1/3}) \tag{8}$$

where Re and Sc denote Reynolds and Schmidt number, respectively.

Energy balance:

$$\frac{\partial}{\partial t}(\rho_a c_i \varepsilon_i T_i) + \frac{\partial}{\partial y}(\rho_a c_i \varepsilon_i u_i T_i) = h_p(T_p - T_i)\frac{6\varepsilon_p}{d_p} + \rho_a k_p(x_p - x_i)\frac{6\varepsilon_p}{d_p}c_v(T_p - T_i) + H_{ib}\varepsilon_b(T_b - T_i) + \rho_a K_{ib}\varepsilon_b(x_b - x_i)c_v(T_b - T_i) + h_w(T_w - T_i)\frac{(1-\varepsilon_p)}{d_{bed}} \tag{9}$$

and interchange coefficient between solid phase and interstitial gas phase:

$$h_p = \frac{k_{tp}}{d_p}(2 + 1.8Re^{1/2}Pr^{1/3}) \tag{10}$$

where Pr is the Prandtl number.

3.3. Solid phase

It is seen from Fig. 3 that the batch drying of solids exhibits constant rate and falling rate periods whose relative magnitudes depend on the system conditions. The drying rate in the constant rate period is enhanced by an increase in temperature. The presence of the constant rate period indicates whether the controlling resistance is limited to external diffusion or to the diffusion of moisture through a layer of crust at the surface. The influence of the temperature is relatively small in a diffusion-controlled process while its effect is slightly higher when the external diffusion controls the process. The rate of drying is affected by the superficial velocity of the drying medium only when external diffusion on the surface of solid particle is a dominant factor in the drying process [8].

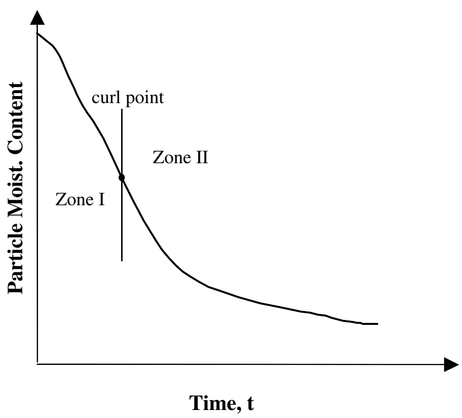

Fig. 3. Drying curve of hazelnut.

3.4. Falling rate period

Solid particles are assumed to be uniform in size, isotropic and approximately spherical in shape. Because of the relatively large size of the particles, it is necessary to consider the gradient of moisture and temperature inside the solid. Therefore, a diffusion type equation is considered for moisture and temperature distributions with appropriate boundary conditions [8]. It is assumed that moisture inside the particle diffuses in the liquid phase to the surface of particles and evaporation takes place only at the surface. The general form of diffusion equation is written as:

$$\frac{\partial M_{\mathrm{p}}}{\partial t} = \nabla \cdot (D \nabla M_{\mathrm{p}}) \tag{11}$$

In a one-dimensional spherical coordinate system and assuming the moisture gradient to be in the radial direction, Eq. (11) becomes:

$$\frac{\partial M_{\mathrm{p}}}{\partial t} = \frac{1}{r^2} \frac{\partial}{\partial r}\left(r^2 D \frac{\partial M_{\mathrm{p}}}{\partial r}\right) \tag{12}$$

with initial and boundary conditions:

$$\begin{aligned}
&t = 0 \quad 0 \leqslant r \leqslant R \quad M_{\mathrm{p}} = M_{\mathrm{pi}}(r) \\
&t > 0 \quad r = 0 \quad \frac{\partial M_{\mathrm{p}}}{\partial t} = 0 \\
&t > 0 \quad r = R \quad \rho_{\mathrm{p}} \Delta V \frac{\partial M_{\mathrm{p}}}{\partial t} = \rho_{\mathrm{a}} k_{\mathrm{p}} A_{\mathrm{p}} (x_{\mathrm{ps}} - x_{\mathrm{i}}) - \rho_{\mathrm{p}} D A_{\mathrm{p}} \frac{\partial M_{\mathrm{p}}}{\partial r}
\end{aligned} \tag{13}$$

The energy equation for the solid particle is given as:

$$\frac{\partial(\rho_{\mathrm{p}} c_{\mathrm{p}} T_{\mathrm{p}})}{\partial t} = \frac{1}{r} \frac{\partial}{\partial r}\left(r^2 k_{\mathrm{tp}} \frac{\partial T_{\mathrm{p}}}{\partial r}\right) \tag{14}$$

where initial and boundary conditions are:

$$\begin{aligned}
&t = 0 \quad 0 \leqslant r \leqslant R \quad T_{\mathrm{p}} = T_{\mathrm{pi}}(r) \\
&t > 0 \quad r = 0 \quad \frac{\partial T_{\mathrm{p}}}{\partial t} = 0 \\
&t > 0 \quad r = R \quad \frac{\partial(\rho_{\mathrm{p}} c_{\mathrm{p}} T_{\mathrm{p}})}{\partial t} = h_{\mathrm{p}} A_{\mathrm{ps}} (T_{\mathrm{i}} - T_{\mathrm{p}}) - \rho_{\mathrm{a}} k_{\mathrm{p}} A_{\mathrm{ps}} (x_{\mathrm{ps}} - x_{\mathrm{i}})(h_{\mathrm{v}} + c_{\mathrm{wa}} T_{\mathrm{p}}) + h_{\mathrm{pw}} A_{\mathrm{ps}} (T_{\mathrm{w}} - T_{\mathrm{p}}) \\
&\qquad - k_{\mathrm{tp}} A_{\mathrm{p}} \frac{\partial T_{\mathrm{p}}}{\partial r}
\end{aligned} \tag{15}$$

In the above equations, diffusion coefficient (D) is function of moisture content and temperature of the solid, which makes the equations coupled. Therefore, they were solved simultaneously in an iterative manner.

3.5. Constant rate period

For this period of drying mass and energy equations are as follows:

$$\frac{\mathrm{d}}{\mathrm{d}t}(M_{\mathrm{p}} \rho_{\mathrm{p}} V_{\mathrm{p}}) = \rho_{\mathrm{a}} k_{\mathrm{p}} A_{\mathrm{p}} (x_{\mathrm{ps}} - x_{\mathrm{i}}) \tag{16}$$

where the initial condition is:

$$\text{at } t = 0 \quad M_p = M_{pi} \tag{17}$$

The energy equation can be written as:

$$\frac{d}{dt}(\rho_p c_p V_p T_p) = h_{pi} A_p (T_i - T_p) - \rho_a k_p A_p (x_{ps} - x_i) h_{fg} + h_{pw} A_{pw} (T_w - T_p) \tag{18}$$

where the initial condition is:

$$\text{at } t = 0 \quad T_p = T_{pi}$$

4. Numerical solution

The set of partial differential equations derived for the modeling of the drying process in the fluidized bed was coupled and solved simultaneously by using the finite volume method [22]. The flow field in the bed was divided into a finite number of control volumes after considering the bed expansion. The conservation equations for all the phases were discretized by using upwind differencing scheme in space while Crank-Nicholson scheme was employed for the temporal differencing to complete the discretization of the governing equations. Results of constant rate period of drying were used as an initial data for falling rate period of the solid particles.

In the first numerical time step, linear system of algebraic equations for whole flow field were solved by using Gauss elimination method with an initial guess and then the first results were used as initial data for next time step. Solution marches into the next time step. This procedure continues until the system converges.

5. Comparison of the experimental results and the model predictions

The experiments have been performed at two different air velocities and temperatures. Moisture content of the material at various times were measured. These experimental data were compared with the results of the mathematical model. Figs. 4–6 show the variation of the moisture content of a particle with time in the experiments and model.

According to experimental data, as shown in Figs. 4–6 temperature has an important effect on the kinetics of drying. Increasing the temperature allows the rate of heat transfer to the product to be increased. At the lower temperature of 40.5 °C the rate of drying was slower than at the temperature of 47 °C. This is reasonable because the mode of the moisture removal is by internal diffusion and the driving force is the temperature difference between the center of the particle and fluidizing air. The greater the temperature, the greater the driving force and hence, a more expedient removal of internal moisture occurs. Again, according to experimental data, as shown in Figs. 4–6 velocity of the air has not played an important role in the rate of drying. In the literature, drying rate is slightly enhanced by an increase in velocity of the air. In this study, increasing the velocity of the air was proved to decrease the drying rate. Because the increasing gas velocity caused the slugging regime to be entered, the drying rate was reduced due to increment of the velocity of the air.

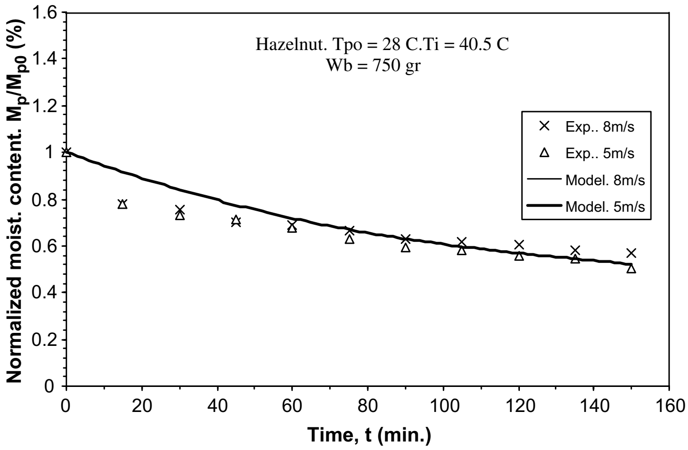

Fig. 4. Comparison of model prediction and experimental results: particle moisture content vs. time with $T_i = 40.5$ °C, $u = 5$ m/s and $u = 8$ m/s.

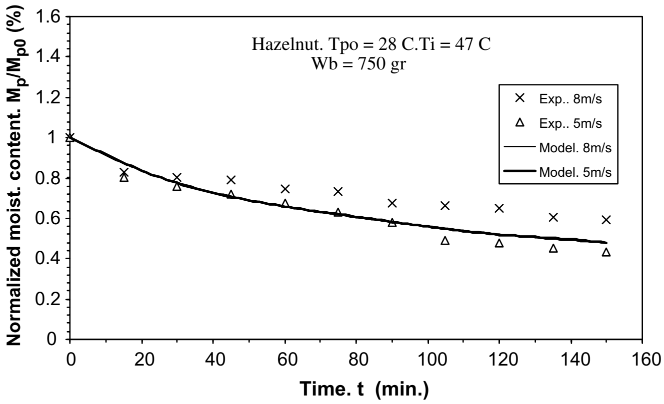

Fig. 5. Comparison of model prediction and experimental results: particle moisture content vs. time with $T_i = 47$ °C, $u = 5$ m/s and $u = 8$ m/s.

Looking at Figs. 4–6, it can be seen that, the effect of velocity of the air are the same on the new harvested and old harvested-dried hazelnuts. There is no difference between drying rate of new harvested and old harvested hazelnuts in the same temperature and velocity of the air conditions.

If the model prediction and experimental data are compared in figures, it is understood that, for old harvested-dried hazelnut (moisture content is <8% on dry basis), there is a good agreement with experimental data and numerical results except for the initial stage of drying which is constant rate period of drying. For new harvested hazelnut, numerical results are close to experimental results but not better than old harvested hazelnut data.

Minimum slugging velocity of hazelnut is up to 6.3 m/s [18]. Therefore, at the end of drying, a small discrepancy between experimental and numerical results was observed in Figs. 4–6 but it can be seen in new harvested hazelnut data, more clearly than for old harvested ones.

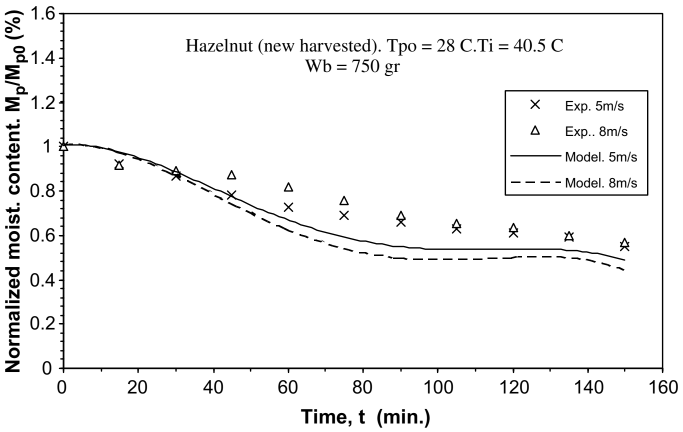

Fig. 6. Comparison of model prediction and experimental results: particle moisture content vs. time with $T_i = 40.5$ °C, $u = 5$ m/s and $u = 8$ m/s.

This model was originally proposed and used by Hajidavalloo and Hamdullahpur [8] for corn and wheat particles. The model has been modified and applied to the problem of drying of hazelnut in a fluidized bed. If all the numerical results of the model were compared with experimental results, it can be said that this model successfully simulates the hydrodynamics of a fluidized bed for the hazelnut drying, with small discrepancies.

6. Conclusion

A new mathematical model proposed by Hajidavalloo and Hamdullahpur [8] was applied to simulate the behavior of the moisture content of hazelnuts in a fluidized bed dryer. Finite volume method has been employed. Also, a laboratory scaled fluidized bed was designed and constructed to investigate the validity of the model. Experimental and model results were compared and evaluated. The suitability of the model for newly harvested and old harvested hazelnuts was investigated. As a result, the model can be used to simulate the hydrodynamics of a fluidized bed for hazelnuts with small discrepancies. At the beginning of drying, the drying rate is very high due to the high surface moisture content, however it decreases with the evaporation of the surface moisture in time.

References

[1] M. Abid, R. Gibert, C. Laguerie, An experimental and theoretical analysis of the mechanisms of heat and mass transfer during the drying of corn grains in a fluidized bed, International Chemical Engineering 30 (4) (1990) 632–641.
[2] S. Bhagya, K.S. Srinivasan, Effect of different methods of drying on the functional properties of enzyme treated groundnut flour, Lebensmittel-Wissenschaft und Technologie 22 (6) (1989) 329–333.
[3] A.N. Chandran, S.S. Rao, Y.B.G. Varma, Fluidized bed drying of solids, AIChE Journal 36 (1) (1990) 29–38.

[4] D.G. Dimattia, P.R. Amyotte, F. Hamdullahpur, Fluidized bed drying of large particles, Transactions of the ASAE 39 (5) (1996) 1745–1750.
[5] D.G. Dimattia, P.R. Amyotte, F. Hamdullahpur, Slugging characteristics of Group D particles in fluidized beds, The Canadian Journal of Chemical Engineering 75 (1997) 452–459.
[6] A.Ç. Erbil, Prediction of the fountain heights in fine particle spouted bed systems, Turkish Journal of Engineering and Environmental Sciences 22 (1998) 47–55.
[7] L.E. Ersoy, M. Köksal, F. Hamdullahpur, Solid holdup and particle velocity measurements in a circulating fluidized bed with secondary air injection, MAMKON'97, ITU Mak. Fak. 1. Mak. Muh. Kongresi, 1997, pp. 17–22.
[8] E. Hajidavalloo, F. Hamdullahpur, Mathematical modeling of simultaneous heat and mass transfer in fluidized bed drying of large particles, in: Proceedings of CSME Form 1998, Volume 1: Symposium on Thermal and Fluids Engineering, Toronto, Canada, 19–22 May 1998.
[9] T. Liang, S.K. Mehra, M.A. Khan, A macadamia nut curing system for improving kernel recovery, Journal of Agricultural Engineering Research 43 (2) (1989) 103–111.
[10] R.G. Moreira, F.W. Bekker-Arkema, Moisture desorption model for nonpareil almonds, Journal of Agricultural Engineering Research 42 (2) (1989) 123–133.
[11] J.R. Puiggali, J.C. Butsale, J.P. Nuderu, The development and use of an equation to describe the kinetics of air drying of hazelnuts, Lebensmittel-Wissenschaft und Technologie 20 (4) (1987) 174–179.
[12] P.P. Thomas, Y.B.G. Varma, Fluidized bed drying of granular food materials, Powder Technology 69 (1992) 213–222.
[13] J.J. Wang, Mathematical modeling of the drying process in fixed bed dryer, Numerical Heat Transfer Part B 24 (1993) 229–241.
[14] M.L. Passos, A.S. Mujumdar, Effect of cohesive forces on fluidized and spouted beds of wet particles, Powder Technology 110 (2000) 222–238.
[15] R.C. Panda, J. Zank, H. Martin, Modeling the droplet deposition behavior on a single particle in fluidized bed spray granulation process, Powder Technology 115 (2001) 51–57.
[16] A. Avci, M. Can, A.B. Etemoglu, A theoretical approach to the drying process of thin film layers, Applied Thermal Engineering 21 (2001) 465–479.
[17] A. Mhimid, S.B. Nasrallah, J.P. Fohr, Heat and mass transfer during drying of granular products simulation with convective and conductive boundary conditions, International Journal of Heat and Mass Transfer 43 (2000) 2779–2791.
[18] A. Topuz, M. Gur, Fluidized bed drying of nuts, The Fourth International Thermal Energy Congress, ITEC 2001, Cesme, Turkiye, 8–12 July 2001.
[19] A. Topuz, Investigation of Heat and Mass Transfer at the Fluidized Bed Drying Process of Hazelnut, PhD Thesis, Sakarya University, Institute of Science and Technology, 2002.
[20] S. Karatas, F.M. Battalbey, Determination of moisture diffusivity of pistachio nut meat during drying, Lebensmittel-Wissenschaft und Technologie 24 (6) (1991) 484–487.
[21] C. Demirtas, Determination of Hazelnut Drying Conditions, PhD Thesis, KTU Institute of Natural Sciences, Trabzon, July 1996.
[22] S.V. Patankar, Numerical Heat Transfer and Fluid Flow, Hemisphere Pub. Co., McGraw-Hill, 1980.